

# Alternative Cr+6-Free Coatings Sliding Against NBR Elastomer

Beatriz Fernandez-Diaz, Raquel Bayón and Amaya Igartua  
*TEKNIKER-IK4*  
Spain

## 1. Introduction

Hexavalent chromium compounds result attractive primarily for industrial activity because they provide manufactured products with enhanced hardness, shininess, durability, color, corrosion resistance, heat resistance, decay resistance and tribological properties. On the other hand, it poses far more health hazards than trivalent chromium. It is a hazardous substance that increases the risk of developing lung cancer if it is inhaled. Ingestion or even simple skin exposure of chromic acid could increase the risk of cancer formation. In this situation, hexavalent chromium is classified by the International Agency for Research on Cancer (IARC) as a known human carcinogen (Group 1) (Working Group on the Evaluation of Carcinogenic Risks to Humans, 1987), where workers have the highest risk of adverse health effects from hexavalent chromium exposure.

Hexavalent chromium has been deeply used in tribological applications being friction and wear reduction also one of the main objectives in sliding mechanical parts for minimizing loss of energy and improving systems performance (Flitney, 2007) (Monaghan, 2008). In the last years, in fact, attention in maintenance costs saving also grow up, therefore a key question is to achieve low levels of friction as well as high wear resistance. In the field of elastomeric materials in 1978 A. N. Gent et al. (Gent, 1978) studied wear of metal by rubber attributing those phenomena at the direct attack upon metals of free radical species generated by mechanical rupture of elastomer molecules during abrasion. It suggested that such studies might lead to new metal texturing processes and surface treatment that can have the double effect of improving the tribological performances and protecting from external agents. Furthermore, coating technology is gaining ground thanks to new available technologies and focusing in particular to the need of using new alternative non toxic surface treatment with equivalent functionality of Cr+6.

The availability of new coating technologies like High Velocity Oxy-Fuel (HVOF) permits to have a wide range of hard coatings, but a deep study of their mechanical and tribological characteristics is needed due to the strong influence of their roughness, hardness, finishing and resistance to wear and corrosion.

HVOF thermal spray technique allows depositing variety of materials (alloys and ceramics). The powdered feedstock of deposition material is heated and accelerated to high velocities in oxygen fuel. The material hits and solidifies as high density well adherent coating material on the sample/ component. HVOF coatings are also strong and show low residual

tensile stress or in some cases compressive stress, which enable very much thicker coatings to be applied than previously possible with the other processes.

An investigation is herein proposed considering NBR (Nitrile butadiene rubber) material sliding against HVOF coated steel rod in order to clarify the influence of the surface characteristics (hardness, roughness and texture) on the tribological measurements. Many times, in addition, the metallic parts need to have good corrosion resistance for protecting them from external hostile atmospheres. A study of the corrosion resistance of the HVOF coatings is then presented, in comparison with the reference Hard Chromium Plating (HCP) treatment.

In this situation, the main objective of this work was to investigate and compare the tribological and corrosion behavior of a reference tribopair NBR/ HCP versus some alternatives based on NBR/ HVOF coatings. These materials combinations simulates contact occurring in sealing systems, where polymer and metallic parts are rubbed each other (Conte, 2006).

## 2. Materials and methodology

### 2.1 Rod coatings

Three different material powders were sprayed by HVOF on a 15-5PH steel rod (diameter 19 mm, length 33 mm): AlBronze, NiCrBSi and WCCoCr. After the HVOF coating process, the cylinders were subjected to different surface modification processes identified as Grinding (G), Superfinishing (F) and Shot Peening (SP). Shot peening was performed with glass balls of diameter in the range of 90- 150  $\mu\text{m}$ , which were injected on the surface of the rods at a pressure of 7 bar and at approximately a distance of 20 mm from the rod. By combining grinding, finishing and shot peening processes it was possible to create different textures on the surface of the coated rods. In addition, reference surface treatment, Hard Chromium Plating (HCP), was also investigated. Coated rods are shown in Fig. 1 where it can be seen that the coatings have been homogeneously deposited on the surface of the rods.

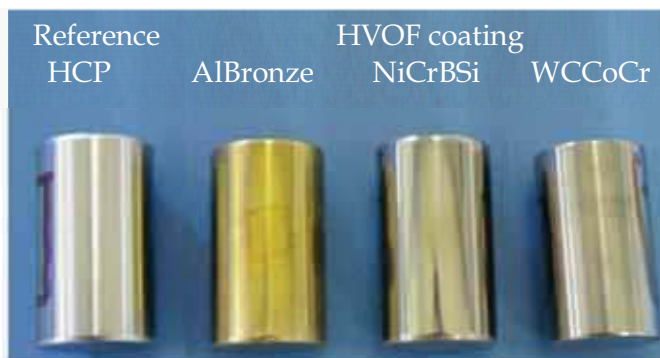


Fig. 1. Coated rod samples. Image corresponds to rods with Grinding process

Table 1 shows some information about hardness and roughness of the tested coated rods. In all the materials “Grinding” and “Grinding + Superfinishing” processes modified the surface of the rods to an averaged roughness of approximately 0.20  $\mu\text{m}$  and 0.04  $\mu\text{m}$ ,

respectively. However, differences were observed when shot peening was applied. WCCoCr material had a high hardness so impacts of microballs did not modify its surface and hence the final surface was very similar to the roughness achieved with the “Grinding” process, that is, 0.28. However, the other two materials (AlBronze and NiCrBSi) were strongly affected by the shots, so final roughnesses were 1.36 and 2.06  $\mu\text{m}$ , respectively. These two last high values have to be considered as rough figures, since the surface of the shot peened coatings was very irregular, so high dispersion of values was obtained.

Rod identification	Coating	Hardness (HV)	Surface texture process	Ra ( $\mu\text{m}$ )
HCP + G (reference)	Hard Chromium Plating	850 $\pm$ 11	Grinding	0.20
AlBronze+G+F	AlBronze (HVOF)	260 $\pm$ 10	Grinding + Superfinishing	0.04
AlBronze+G			Grinding	0.22
AlBronze+SP+G			Shot peening+ Grinding	1.36
NiCrBSi+G+F	NiCrBSi (HVOF)	745 $\pm$ 15	Grinding +Superfinishing	0.04
NiCrBSi+G			Grinding	0.16
NiCrBSi+SP+G			Shot peening+ Grinding	2.06
WCCoCr+G+F	WCCoCr (HVOF)	1115 $\pm$ 92	Grinding +Superfinishing	0.03
WCCoCr+G			Grinding	0.23
WCCoCr+SP+G			Shot peening+ Grinding	0.28

Table 1. Tested coated rods

Fig. 2 to Fig. 4 show the cross section of the HVOF coated rods where structure can be examined. For this characterization, rods with shot peening process were selected in order to analyze the deformation suffered by the coating after the glass impacts. The thickness of the coatings was in the range of 120-150  $\mu\text{m}$ . Neither pores nor cracks in the interface of the coating were found in the coatings, which improves corrosion resistance and facilitates proper bonding, respectively. However, the analysis of the SEM images evidences the presence of some irregularities in the coatings which were analyzed in detail.

In the WCCoCr coating (Fig. 2) Nickel traps form some clusters of material. These clusters could come from previous processes where Nickel was deposited (for example in the preparation of the NiCrBSi coating). It was also identified alumina particles between the substrate and the coating (darker area in Fig. 2) which could come from the machining process. No evidence of craters was present on the surface of the coatings. It seemed that the hard nature of this coating (1115 $\pm$ 92 HV) made difficult the creation of craters on its surface. The NiCrBSi coating (Fig. 3) had many clusters of material particles. The pale clusters corresponded to Molybdenum, also detected in the surface of this rod; the dark polygonal clusters corresponded again to alumina. The alumina was detected not only between

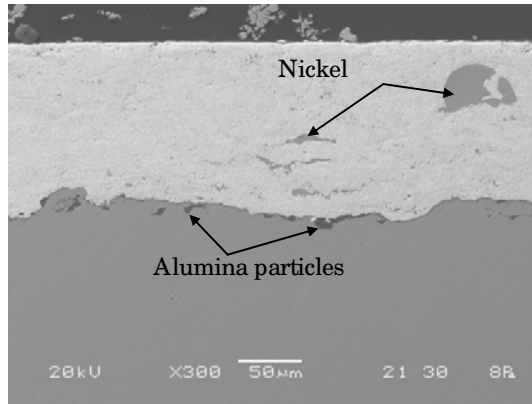


Fig. 2. WCCoCr + SP+ G coating

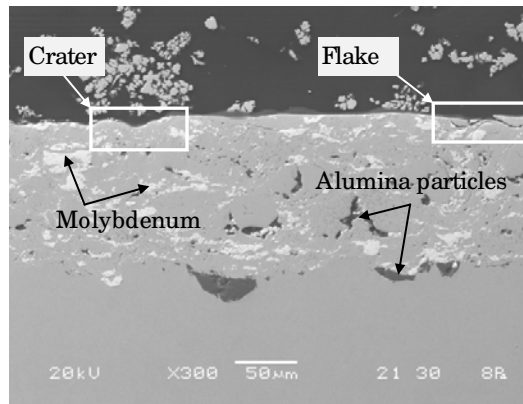


Fig. 3. NiCrBSi + SP+ G coating

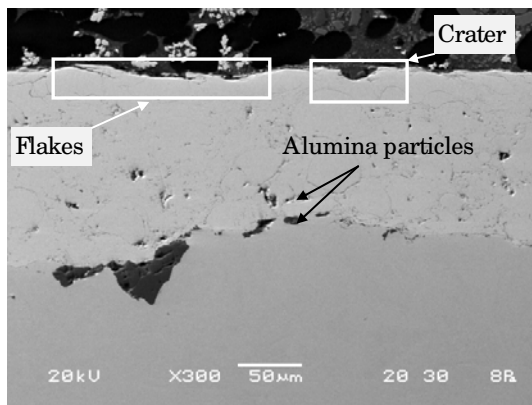


Fig. 4. Al Bronze + SP+ G coating

the substrate and the coating, but also in the matrix of the coating. In this case, shots of the glass balls did perform craters on the coating, increasing then the roughness of the coating till  $2.06\ \mu\text{m}$ . In some areas of the surface of the coating it was appreciated flakes-like irregularities which could had been provoked during the finishing process. These non homogeneous features under severe working conditions could accelerate the fail of the coating.

The superficial appearance of the AlBronze coating (Fig. 4) was similar to the NiCrBSi coating. It showed high roughness ( $R_a=1.36\ \mu\text{m}$ ) because of the combination of its relatively low hardness (260 HV) and the craters performed during the shot peening; flake-like cracks and alumina clusters were again found within the coating.

## 2.2 NBR elastomer

NBR elastomer samples were obtained from real seals, and had a hardness of  $85\pm 1\ \text{ShA}$ . The material was analyzed by Thermogravimetry Analysis (TGA) and Scanning Electro Microscopy with Energy Dispersive X-ray Spectroscopy (SEM-EDS) techniques. The composition of the tested NBR is shown in Table 2. The analysis of the inorganic part revealed the presence of Magnesium Silicate (talc), Sulphur and Zinc Oxide. Magnesium Silicate is used as compounding material, Sulphur acts as vulcanization agent and Zinc Oxide is used for activating this process.

Component	Quantity (% in weight)
Elastomer and plasticizers	49
Carbon black	46
Inorganic filler	5

Table 2. Composition of the NBR rubber

## 2.3 Tribological tests

Friction and wear tests were carried out using the cylinder on plate configuration (Fig. 5). Coated rods were put in contact against flat sample of NBR under sliding linear reciprocating conditions. Contacting surfaces were lubricated using AeroShell Fluid 41 hydraulic mineral oil.

During the test, the coated rod was linearly reciprocated at a maximum linear speed of  $100\ \text{mm/s}$  with a stroke of  $2\ \text{mm}$ . Testing normal load was applied gradually in order to soften the contact between the metallic rod and the rubber sample: during the first  $30\ \text{s}$  it was set a normal load of  $50\ \text{N}$  and then a ramp of load was applied to reach  $100\ \text{N}$ , the testing normal load. Tests had a duration of  $30\ \text{min}$ .

Specimens were located in a climate chamber to set temperature and relative humidity at  $25\ ^\circ\text{C}$  and  $50\ \%\text{RH}$ , respectively. Each material combination was tested at least twice in order to evaluate the dispersion of the results.

It was recorded the evolution of the coefficient of friction through time and, after the tests, surface damage on the specimens was analyzed by optical microscopy. It was also considered the evaluation of the mass loss but no significant results were obtained, so it was not reported.

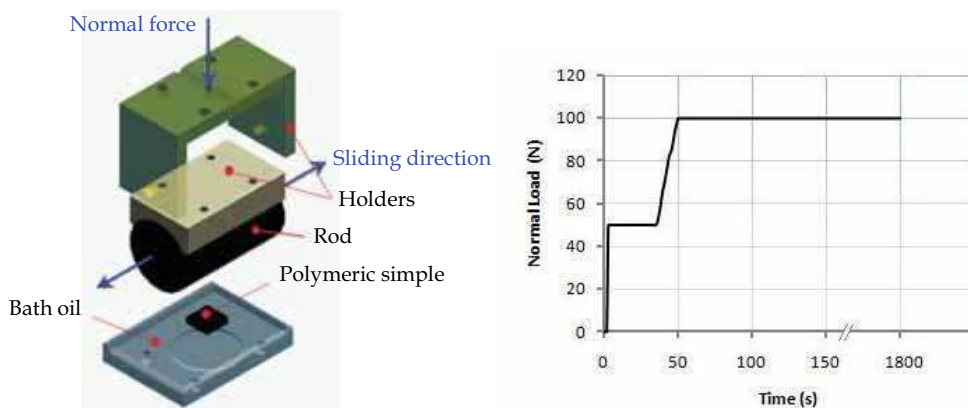


Fig. 5. Scheme of the testing arrangement (Cylinder on Plate configuration) (a) and load history (b)

## 2.4 Corrosion tests

Corrosion tests were performed in a conventional electrochemical cell of three electrodes. The reference electrode used for these measurements was a silver/ silver chloride electrode (SSC, 0.207V vs SHE), the counter electrode was a platinum wire and the working electrode was the studied surface in each case. The exposed area of the samples was 1.47 cm<sup>2</sup>. Tests were done at room temperature and under aerated conditions. The aggressive media used was NaCl 0.06M. The electrochemical techniques applied for the corrosion behaviour study were electrochemical impedance spectroscopy in function of immersion time (4 and 24 hours of immersion) and potentiodynamic polarization.

On the other hand, impedance measurements were performed at a frequency range between 100 kHz and 10 mHz (10 freq/ decade) with a signal amplitude of 10 mV. Polarization curves were registered from -0.4V versus open circuit potential (OCP) and 0.8 V vs OCP at a scan rate of 0.5mV/ s.

## 3. Friction and wear behaviour of hard coatings and rubber material

The evolution of friction coefficient through time for the different rods is shown in Fig. 6. The steady-state of the coefficient of friction was reached from the beginning of the tests, that is, the running-in phase is really short. The high values during the first seconds corresponded to the loading phase since the setting of the testing normal load was reached after 50 s.

Considering the mean values of the friction curves it was found that in general, for the three HVOF coatings, the lower the averaged roughness, the higher the mean friction coefficient, independently of the material of the coating (Fig. 7). The effect of reducing roughness by mechanical surface treatments revealed that lowering rod roughness did not promote the formation of the lubrication film in the interphase rod/ rubber, resulting in friction force increment. This general tendency was not followed by the AlBronze coating. This material had the lowest hardness so it was very affected by the shot peening process, which generated a very irregular surface with unbalanced tribological effect.

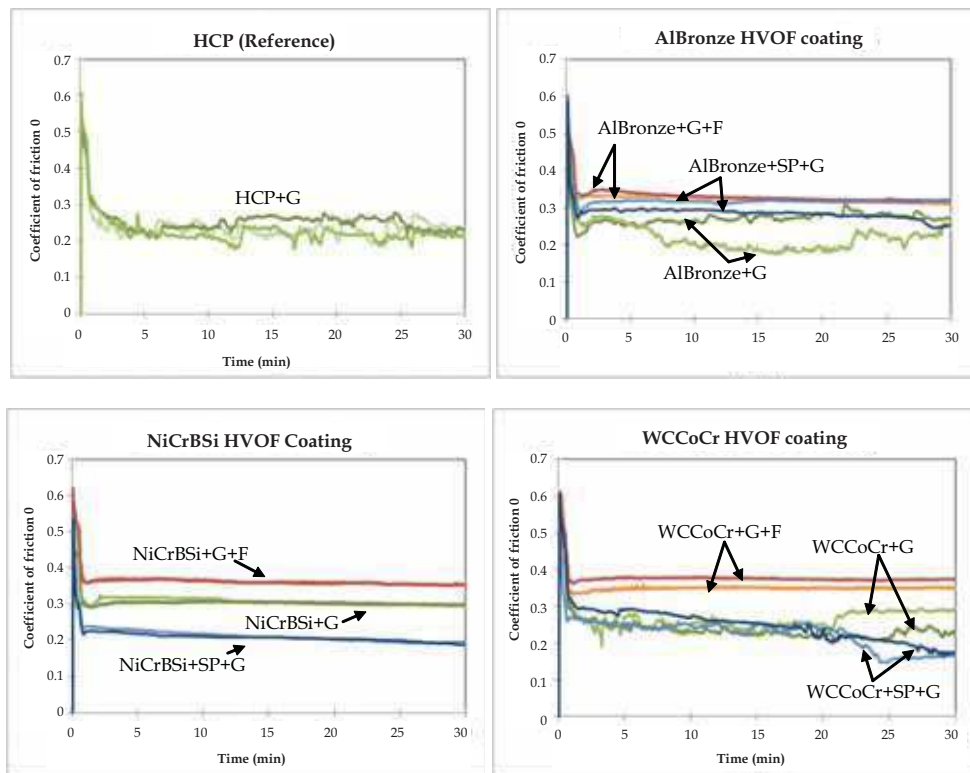


Fig. 6. Friction curves

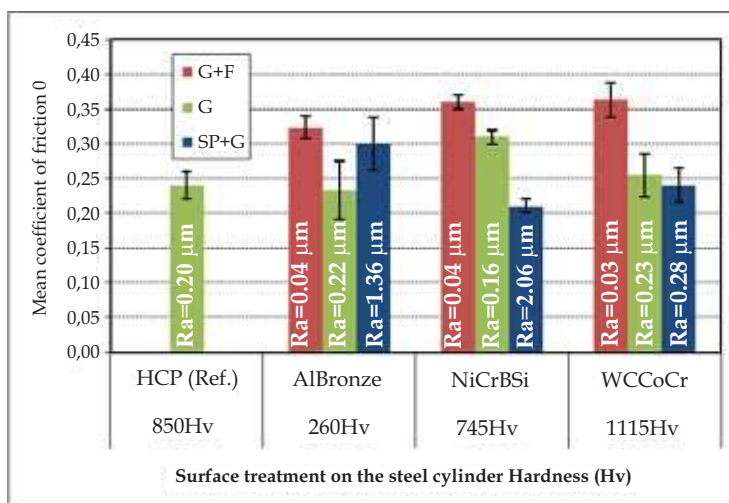


Fig. 7. Mean coefficient of friction, averaged roughness and hardness

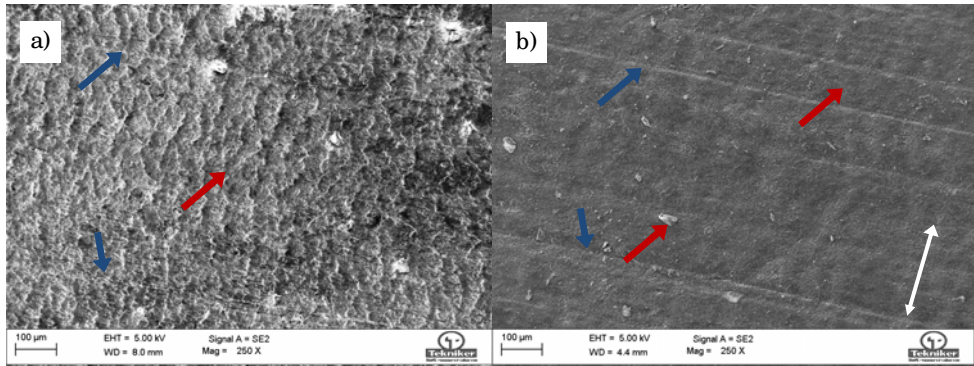


Fig. 8. Not tested area on the NBR elastomeric samples (a) and worn area after tests against HCP+G reference material (b). White arrow indicates sliding direction. Blue arrows indicate straight marks from the mould. Red arrows indicate points where X-Ray analysis was done

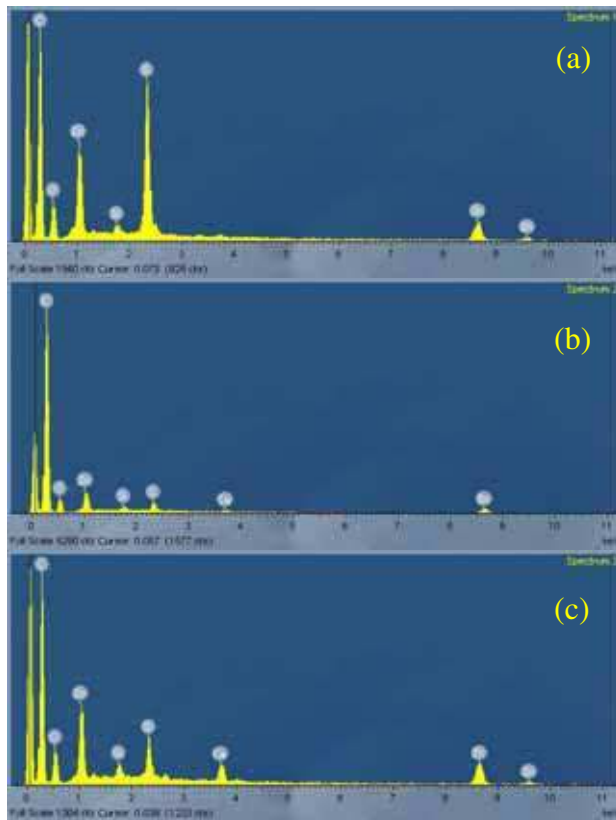


Fig. 9. X-Ray microanalysis on the NBR sample: not tested surface (a), plain worn area (b) and particle on the worn surface (c)



The coated rods did not suffer damage as consequence of the contact with the relatively soft rubber sample; the lubrication film protected effectively the metallic surfaces. On the other hand, strong influence of the counterbody was observed when analyzing the wear behaviour of the NBR elastomers.

An overview of the SEM images showing the surface damage on the surface of the NBR samples revealed different wear behaviour depending on the tested counterbody. The initial surface texture of the NBR sample had a flake-like shape (Fig. 8 (a)), a texture acquired during the moulding phase of the elastomeric sample. Straight lines were also observed, again a replica of the texture of the mould. As observed in Fig. 8 (b) the reference cylinder coating HCP softened this texture by reducing the microscopic roughness. However, straight lines from the mould remained still visible. Particles on the worn area were analyzed by X-Ray. Spectrum of Fig. 9 (c) indicated they were rubber with a significant amount of Sulphur and Zinc. These elements corresponded to the components used in the vulcanization process of the rubber. They tend to emigrate to surface of the NBR sample and thus, they remain within the matrix of the detached wear particles. Important presence of these two elements was found on the untested area (Fig. 9 (a)); contrary, the plain worn area had less quantity of these elements as observed in Fig. 9 (b), since the successive cycles removed the upper film of the NBR sample.

In relation to the tests with the HVOF coated rods, the intensity of the surface damage on the NBR sample was very influenced by the surface texture of the rod. Rods with high roughness (AlBronze+SP+G and NiCrBSi+SP+G) produced important abrasion marks in the sliding direction as observed in Fig. 10 (c) and Fig. 11 (c). With rods of lower roughness this phenomenon was still present, but with lower intensity (Fig. 10 (b) and Fig. 12 (c)). Schallamach waves (Schallamach, 1971) perpendicular to the sliding direction were observed on the NBR after the test with the AlBronze+G (Fig. 10 (b)), which indicated that micro-bonding between contacting surfaces occurred. This material produced light surface damage on the NBR when the surface roughness was low according to the Superfinishing process (Fig. 10 (a)). There is still present the flake-like shape of the texture of the untested rubber, as well as the straight lines from the mould. The same behaviour was observed with the WCCoCr+G+F rod as shown in Fig. 12 (a). On the other hand, the NiCrBSi alloy with the G+F and G processes roughened the NBR surface in very similar way; the rubber failed by cracking and fatigue phenomena.

#### 4. Corrosion resistance of coatings

Open circuit measurements registered during the initial 5000 s of immersion in the electrolyte appear in Fig. 13. The potential in case of reference chromed sample differs from the rest of coatings showing a more stable and noble open circuit potential.

After the first 4 hours of immersion an electrochemical impedance spectroscopy was performed on each surface to evaluate the electrochemical response of the coatings to the selected aggressive media. In this study, EIS (Electrochemical Impedance Spectroscopy) was employed to detect the pinholes in the coatings proposed and assessed their effect on the system corrosion behaviour over longer immersion times. Because of that, a second EIS was additionally measured on each sample after 24 hours of exposure to the aggressive electrolyte. Fig. 14 shows the impedance diagrams registered at 4 h and 24 h of immersion for each coating.

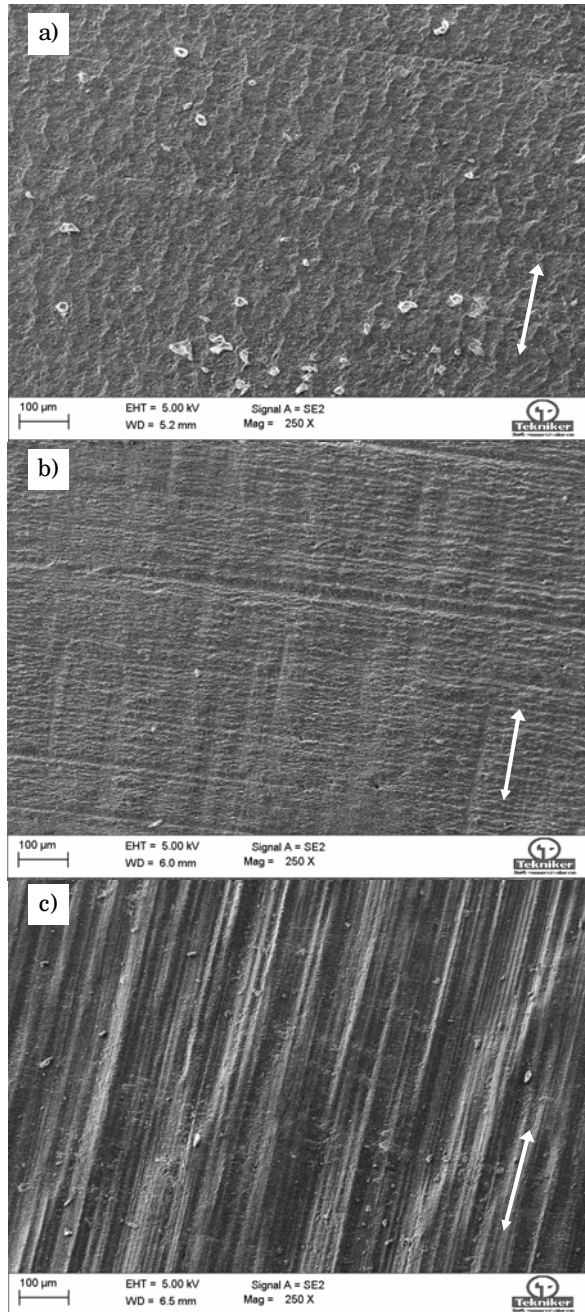


Fig. 10. Worn areas on NBR elastomeric samples against AlBronze coatings: G+F (a), G (b) and SP+G (c). White arrows indicate sliding direction

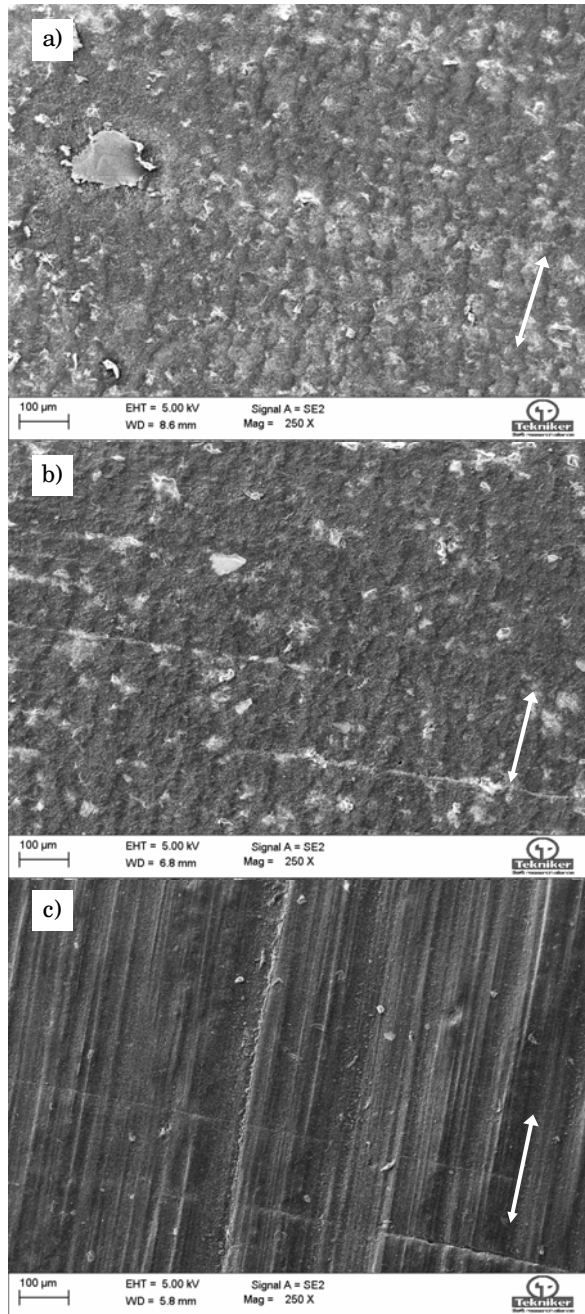


Fig. 11. Worn areas on NBR elastomeric samples against NiCrBSi coatings: G+F (a), G (b) and SP+G (c). White arrows indicate sliding direction

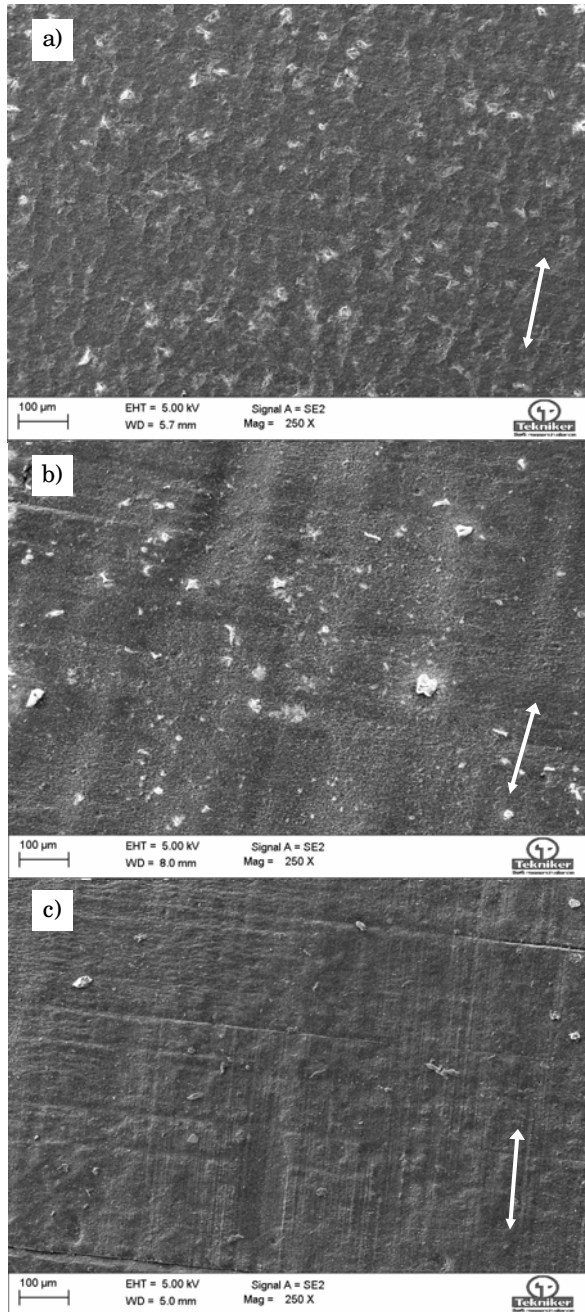


Fig. 12. Worn areas on NBR elastomeric samples against WCCoCr coatings: G+F (a), G (b) and SP+G (c). White arrows indicate sliding direction

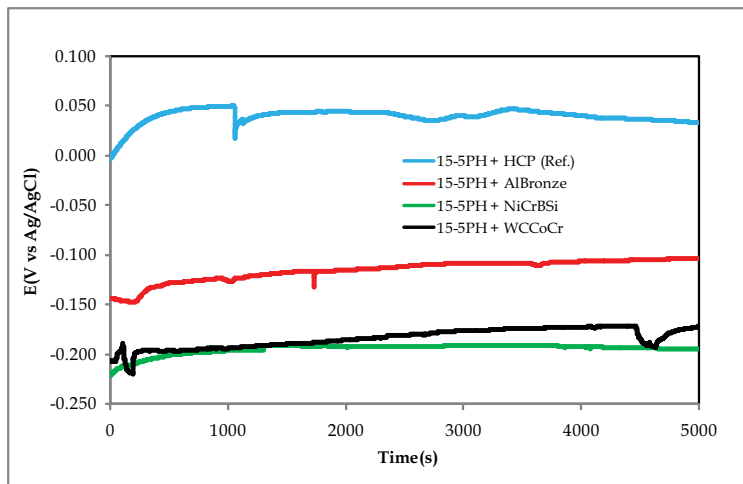


Fig. 13. Open circuit potential measurements of coated rods in NaCl 0.06M

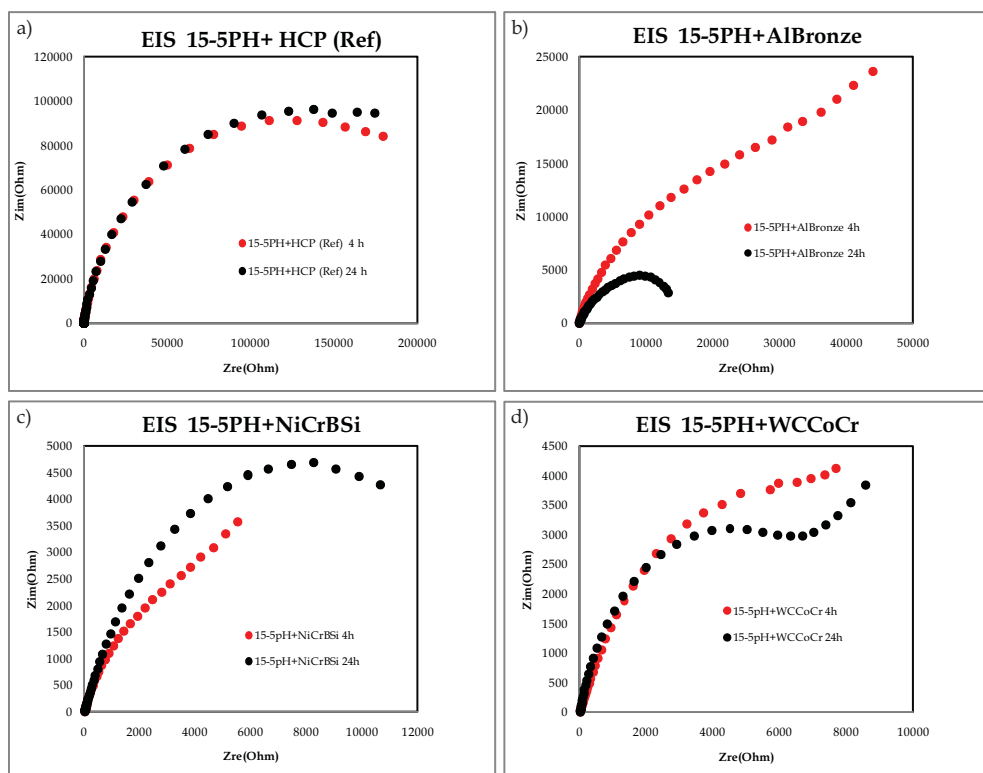


Fig. 14. Impedance diagrams at 4 h and 24 h of immersion in NaCl 0.6M; a) chromed reference, b) AlBronze coating; c) NiCrBSi coating and d) WCCoCr coating

Fig. 15 gives the Bode plots from the coated samples over the two immersion times in NaCl. According to the impedance diagram, after 4 h immersion, only one semi-circle was shown in all cases, corresponding to the coatings time constant. Low immersion periods were too short to reveal any contribution of the 15-5PH substrate. When the immersion period was increased to 24 h, the phase shift was different to that of 4 h in all alternative coatings, except in case of reference HCP film, whose Bode spectra remains stable and very similar to the first one registered at 4 h of exposure time.

At 4 h of immersion time, all coatings showed diffusion processes in the low frequency range and the experimental data could be fitted by using the equivalent circuit (A) drawn in Fig. 16. The electrochemical parameters obtained using this circuit are listed in Table 3. In this case, CPE1 is the constant phase element of the coating (CPE-c) which impedance can be written as  $Z_{CPE} = 1 / Y_0(i\omega)^n$ . R1 is the charge transfer resistance ( $R_{ct}$ ) in the interface coating/ electrolyte and W is the diffusion element ( $Z_w$ ).

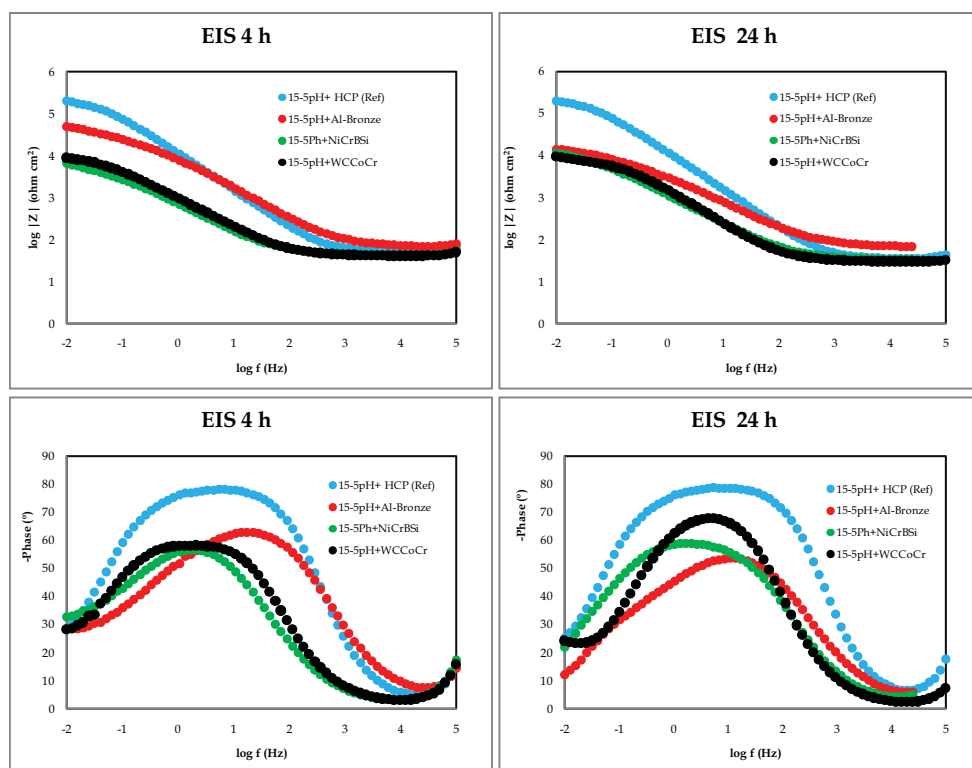


Fig. 15. Impedance data (Bode diagrams) of reference and alternative coatings for 15-5PH alloy at 4 h and 24 h of immersion in NaCl 0.06M

After 24 h of immersion, impedance data of the three alternative coatings (AlBronze, NiCrBSi and WCCoCr) presented two time constants due to the contribution of the substrate through the coatings micropores or defects. In this case, the experimental data could be fitted with the equivalent circuit (B) where CPE-c corresponds to CPE1, the constant phase

element of the coating,  $R_2$  is  $R_{po}$ , the resistance through the coating pores, CPE-s is CPE-2, the constant phase element of the substrate and  $R_{ct}$  corresponds to  $R_2$ , the charge transfer resistance in the interface substrate/ electrolyte.

	HCP		AlBronze		NiCrBSi		WCCrCr	
Time (h)	4	24	4	24	4	24	4	24
$E_{oc}$ (V)	0.025	0.050	-0.087	-0.183	-0.192	-0.258	-0.171	-0.174
$R_s$ ( $\Omega \cdot \text{cm}^2$ )	68.2	46.6	89.3	88.2	56.9	42.9	52.6	39.1
$R_1$ ( $\text{K}\Omega \cdot \text{cm}^2$ )	238.0	242.1	38.2	11.26	6.7	16	12.1	24.9
Y0-CPE-1 ( $10^{-4}\text{F}/\text{cm}^2$ )	0.127	0.123	0.203	0.566	2.751	3.337	1.973	10.21
N1	0.885	0.888	0.742	0.687	0.716	0.668	0.73	0.691
$Z_w$ ( $10^{-3} \Omega^{-1} \cdot \text{cm}^{-2} \cdot \text{s}^{1/2}$ )	0.039	0.049	8.769	/	0.701	/	0.845	/
$R_2$ ( $\text{K}\Omega \cdot \text{cm}^2$ )	/	/	/	9.9	/	5.9	/	8
Y0-CPE-2 ( $10^{-4}\text{F}/\text{cm}^2$ )	/	/	/	1.646	/	3.681	/	1.165
$n_2$	/	/	/	0.762	/	0.758	/	0.843

Table 3. Electrochemical parameters obtained from EIS tests using the equivalent circuits of Fig. 16 in NaCl 0.06M

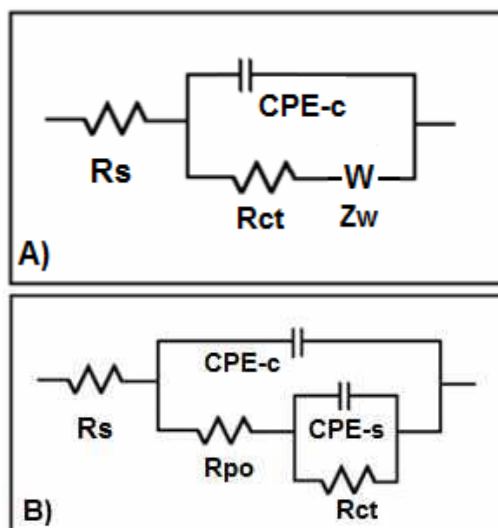


Fig. 16. Equivalent circuits used to simulate impedance experimental data. Circuit A) used in all cases at 4 hours of immersion time, and at 24h in case of chromed reference sample. Circuit B) used at 24h of immersion time for the three alternative coatings: AlBronze, NiCrBSi and WCCoCr

According to this results, it was seen that the HCP coating was a very good reference for corrosion protection in chloride media since it showed the most constant and stable behaviour after 24 hours of immersion time, as well as high corrosion resistance in comparison to the other alternative coatings.

After 24 hours of exposure, a potentiodynamic polarization curve was performed on the different coated rods. The potential-current curves are exposed in Fig. 17. The results of polarization tests were in agreement with impedance measurements. Chromed rod showed the lowest corrosion current over the whole potential range analyzed, whereas in the case of AlBronze and NiCrBSi coatings the current progressively increased when potential went to more anodic values which involved a more active behaviour in these cases. WCCoCr coating showed more stable and lower corrosion current than the other two alternatives but the corrosion resistances were worst than those measured in case of reference coating (Table 4).

	E <sub>corr</sub> (V)	I <sub>corr</sub> (10 <sup>-6</sup> A)	R <sub>p</sub> (KΩ)
15-5PH+HCP (Ref)	-0.095	0.13	417
15-5PH+AlBronze	-0.209	12.50	7
15-5PH+NiCrBSi	-0.269	1.79	21
15-5PH+WCCoCr	-0.271	1.40	38

Table 4. Tafel analysis of potential-current curves

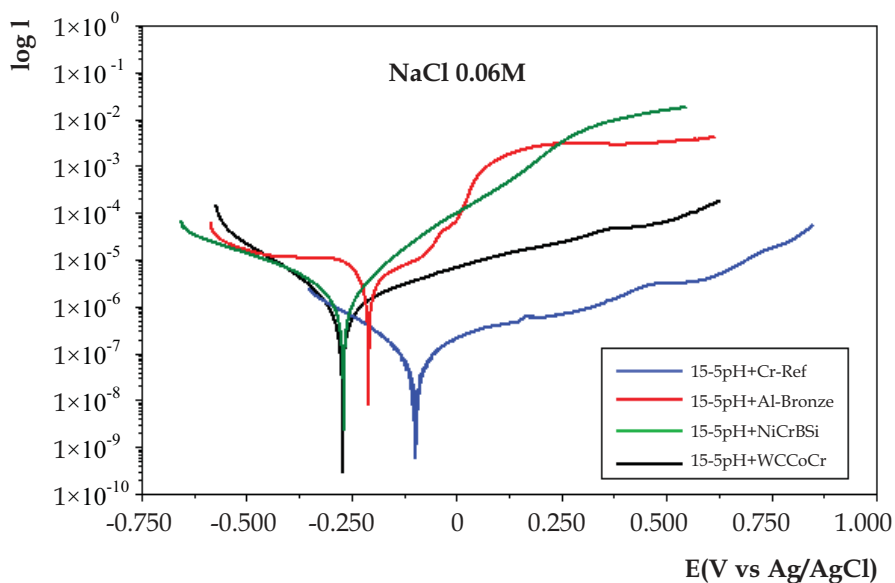


Fig. 17. Potentiodynamic polarization curves of coated 15-5PH samples after 24 hours of immersion in NaCl 0.06M



## 5. Conclusions

Tribological tests under lubricated conditions were performed in order to compare the friction and wear behaviour of reference HCP and some alternative HVOF coatings applied on 15-5PH steel rods, sliding in against NBR elastomer. Additionally a corrosion resistance study was carried out on the coated rods. According to the obtained results the following conclusions can be drawn:

- In terms of friction, in general it was seen that for the studied HVOF coatings, the lower the averaged roughness, the higher the mean friction coefficient, independently of the material of the coating. In addition, wear suffered by the NBR elastomer was very sensitive to the surface texture on the rod, and, rods with elevated roughness generated not acceptable surface damage on the rubber. So, surprisingly, those NBR samples with lower surface damage did not corresponded with tests with low coefficients of friction. This phenomenon suggested significant temperature rise in the contact.
- The corrosion tests revealed that the reference HCP surface coating was a very good reference for corrosion protection and had better behaviour than the proposed HVOF coatings. However, it must be pointed out that obtained values indicated good behaviour of these coatings.
- Considering the tribological and corrosion results, it can be said that the AlBronze+G HVOF coating could be considered as good alternative to replace the reference HCP treatment since it generated an equivalent friction and produced an acceptable damage on the surface of the elastomeric material. Additionally, its corrosion response was good enough for protecting the substrate material.

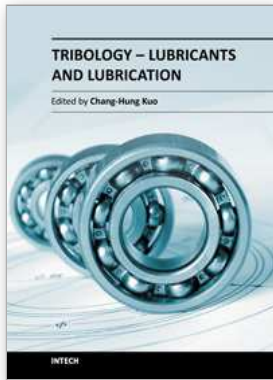
## 6. Acknowledgment

The authors would like to acknowledge the EU for their financial support (KRISTAL: Knowledge-based Radical Innovation Surfacing for Tribology and Advanced Lubrication, Contract Nr.: NMP3-CT-2005-515837 ([www.kristal-project.org](http://www.kristal-project.org))). We also wish to acknowledge Mr. A. Straub (Liebherr Aerospace Lindenberg GmbH, Lindenberg, Germany) and Dr. M. Meyer from EADS, Ottobrunn, Germany) for their valuable collaboration on this research. Finally, we thank our colleagues Xana Fernández, Gemma Mendoza, Roberto Teruel, Virginia Sáenz de Viteri, Elena Fuentes and Marcello Conte for their support in the experimental work.

## 7. References

- Conte, M. (2006), Interaction between seals and counterparts in pneumatic and hydraulic components. *PhD Thesis* (June 2009)
- Flitney, B. (2007). Alternatives to chrome for hydraulic actuators. *Sealing Technology*, Vol 2007, Issue 10, (October 2007), pp.8-12
- Gent A.N., Pulford C.T.R. (1978). Wear of steel by rubber. *Wear*, Vol. 49, Issue 1, (July 1978), pp. 135-139
- Monaghan, K. J. & Straub, A. (2008). Comparison of seal friction on chrome and HVOF coated rods under conditions of short stroke reciprocating motion. *Sealing Technology*, Vol 2008, Issue 11, (November 2008), pp. 9-14

Schallamach, A. (1971), How does rubber slide?, *Wear*, Vol. 17, Issue 4, pp.301–312  
Working Group on the Evaluation of Carcinogenic Risks to Humans (1987), *IARC Monographs on the evaluation of the Carcinogenic Risks to Humans*, Supplement 7, International Agency for Research on Cancer (IARC), ISBN 9283214110, Lyon



## **Tribology - Lubricants and Lubrication**

Edited by Dr. Chang-Hung Kuo

ISBN 978-953-307-371-2

Hard cover, 320 pages

**Publisher** InTech

**Published online** 12, October, 2011

**Published in print edition** October, 2011

In the past decades, significant advances in tribology have been made as engineers strive to develop more reliable and high performance products. The advancements are mainly driven by the evolution of computational techniques and experimental characterization that leads to a thorough understanding of tribological process on both macro- and microscales. The purpose of this book is to present recent progress of researchers on the hydrodynamic lubrication analysis and the lubrication tests for biodegradable lubricants.

### **How to reference**

In order to correctly reference this scholarly work, feel free to copy and paste the following:

Beatriz Fernandez-Diaz, Raquel Bayón and Amaya Igartua (2011). Alternative Cr+6-Free Coatings Sliding Against NBR Elastomer, Tribology - Lubricants and Lubrication, Dr. Chang-Hung Kuo (Ed.), ISBN: 978-953-307-371-2, InTech, Available from: <http://www.intechopen.com/books/tribology-lubricants-and-lubrication/alternative-cr-6-free-coatings-sliding-against-nbr-elastomer>

# **INTECH**

open science | open minds

### **InTech Europe**

University Campus STeP Ri  
Slavka Krautzeka 83/A  
51000 Rijeka, Croatia  
Phone: +385 (51) 770 447  
Fax: +385 (51) 686 166  
[www.intechopen.com](http://www.intechopen.com)

### **InTech China**

Unit 405, Office Block, Hotel Equatorial Shanghai  
No.65, Yan An Road (West), Shanghai, 200040, China  
中国上海市延安西路65号上海国际贵都大饭店办公楼405单元  
Phone: +86-21-62489820  
Fax: +86-21-62489821

© 2011 The Author(s). Licensee IntechOpen. This is an open access article distributed under the terms of the [Creative Commons Attribution 3.0 License](#), which permits unrestricted use, distribution, and reproduction in any medium, provided the original work is properly cited.